

Revised WMAP constraints on neutrino masses and other extensions of the minimal Λ CDM model

Jostein R. Kristiansen* and Øystein Elgarøy†

Institute of Theoretical Astrophysics, University of Oslo, Box 1029, 0315 Oslo, NORWAY

Hans Kristian Eriksen‡

Institute of Theoretical Astrophysics, University of Oslo, Box 1029, 0315 Oslo, NORWAY

Centre of Mathematics for Applications, University of Oslo, Box 1053 Blindern, 0316 Oslo, NORWAY

Jet Propulsion Laboratory, 4800 Oak Grove Drive, Pasadena CA 91109, USA and

California Institute of Technology, Pasadena, CA 91125, USA

(Dated: June 17, 2018)

Recently, two issues concerning the three-year Wilkinson Microwave Anisotropy Probe (WMAP) likelihood code were pointed out. On large angular scales ($l \lesssim 30$), a sub-optimal likelihood approximation resulted in a small power excess. On small angular scales ($l \gtrsim 300$), over-subtraction of unresolved point sources produced a small power deficit. For a minimal six-parameter cosmological model, these two effects conspired to decrease the value of n_s by $\sim 0.7\sigma$. In this paper, we study the change in preferred parameter ranges for extended cosmological models, including running of n_s , massive neutrinos, curvature, and the equation of state for dark energy. We also include large-scale structure and supernova data in our analysis. We find that the parameter ranges for α_s , Ω_k and w are not much altered by the modified analysis. For massive neutrinos the upper limit on the sum of the neutrino masses decreases from $M_\nu < 1.90\text{eV}$ to $M_\nu < 1.57\text{eV}$ when using the modified WMAP code and WMAP data only. We also find that the shift of n_s to higher values is quite robust to these extensions of the minimal cosmological model.

I. INTRODUCTION

The temperature fluctuations in the cosmic microwave background (CMB) radiation have proved to be the single most important cosmological observable we have today, and the high-precision full-sky maps provided by the Wilkinson Microwave Anisotropy Probe (WMAP) play a very important role in the determination of cosmological parameters and preferred cosmological models [1]. One of the most important conclusions both from the WMAP data alone, and from joint analyses including other cosmological observables, is that a simple six-parameter flat Λ CDM model fits the data very well, and that extended models with additional free parameters do not improve the fit significantly.

Because of the great impact of WMAP data, the 3-year data analysis from the WMAP team has been subject to exhaustive cross-checking. In particular, in refs. [2] and [3] two noticeable issues with the likelihood code as first presented by the WMAP team were pointed out. First, the likelihood approximation used between $13 \leq l \lesssim 30$ appears to be inadequate, effectively resulting in a $\sim 5\%$ power excess in this range compared to an exact treatment. Second, the amplitude for the unresolved point source spectrum used by the WMAP team was found to over-subtract the actual contribution in the data, leading to a power deficit at high l 's.

In [3], the effect of these discrepancies were studied for a minimal six-parameter cosmological model. This was done both for WMAP data only, and with additional CMB data from small-scale experiments. Their main finding was an increase in n_s , lowering the significance of $n_s \neq 1$ from $\sim 2.7\sigma$ to $\sim 2.0\sigma$.

In this paper we consider the effect on extended cosmological models. We study how the modified WMAP likelihood affects the preferred ranges of the running of the scalar spectral index, the cosmological neutrino mass limits, spatial curvature, and the equation of state for dark energy. We have also taken into account large-scale structure (LSS) and type 1a supernovae (SNIa) data sets, to see whether the shifts in preferred parameter ranges survive a more thorough cosmological analysis. Further, we consider whether the shift of n_s to larger values is robust to changes in cosmological models and data sets.

In the next section, we review both the methods and data we use. In Section III, we report and comment upon our results, before summarizing and concluding in Section IV.

II. DATA AND METHODS

A. WMAP data

The WMAP experiment is a NASA-funded satellite mission designed to measure the CMB temperature anisotropies over the full sky at five frequencies between 23 and 94 GHz with unprecedented angular resolution and sensitivity. These measurements allow for an accurate determination of the angular CMB power spectrum

*Electronic address: j.r.kristiansen@astro.uio.no

†Electronic address: oelgaroy@astro.uio.no

‡Electronic address: h.k.k.eriksen@astro.uio.no

for angular scales between, say, $l = 2$ and 800 with three years of observations.

Estimation of this spectrum and the corresponding likelihood function is a multi-step process. First, sky maps are generated from the raw satellite data, and the instrumental noise is estimated. Second, contaminants in the form of galactic and extra-galactic foregrounds are removed from the sky maps, and severely contaminated regions are removed completely from further analysis. Third, the power spectrum is estimated with some algorithm, usually trading off computational efficiency against accuracy. Fourth, a connection is made between the power spectrum and the likelihood.

These steps are all described in detail for the three-year WMAP data release in ref. [4]. The main result of these efforts is a user-friendly Fortran 90 code that for an input power spectrum outputs the corresponding likelihood value. In principle, this piece of code may be used as a “black box”.

However, some care is warranted. In particular, two points were noted in ref. [2]. First, there is a $\sim 5\%$ discrepancy between the temperature likelihood approximation used by the WMAP team and an exact evaluation for $l \lesssim 30$. Second, there is a $\sim 60 \mu\text{K}^2$ discrepancy between the two spectra observed at 61 and 94 GHz. The former is primarily due to estimator approximations and secondarily to residual foregrounds. The latter issue was later partly explained in terms of an excessive point source correction applied to the WMAP spectrum [3].

In the present paper, we therefore use two versions of the WMAP likelihood. The first version is simply the official code as provided on LAMBDA[25]. The second version includes two modifications to this code: At $l \leq 30$, we replace both the WMAP pixel-based likelihood and the pseudo- C_l -based likelihood with an exact Gibbs sampling based estimator [2]. Then the spectrum amplitude of unresolved point sources (relative to 41 GHz) is adjusted from $A = 0.017 \mu\text{K}^2\text{sr}$ to $A = 0.011 \mu\text{K}^2\text{sr}$ [3]. We do not marginalize over the SZ (Sunyaev-Zeldovich) amplitude in our analyses.

B. Other data sets used

In our analysis we use additional CMB data, data from LSS surveys, SNIa data and additional priors on the Hubble parameter and baryon content of the universe.

1. Other CMB observations

To probe a larger range of angular scales in the CMB power spectrum we use CMB data from ACBAR [5] and BOOMERanG [6, 7, 8].

2. Large scale structure

Large scale structure surveys probe the matter distribution in the universe by measuring the galaxy-galaxy power spectrum $P_g(k, z) = \langle |\delta_g(k, z)|^2 \rangle$. In the linear perturbation regime it is expected that this galaxy-galaxy spectrum is proportional to the total matter power spectrum, P_m , through the simple relation $P_g = b^2 P_m$, where b is called the bias parameter.

There are two galaxy surveys of comparable size, namely the 2 degree Field Galaxy Redshift Survey (2dF) [9] and the Sloan Digital Sky Survey (SDSS) [10]. In our analysis we use data from both these surveys.

3. Type 1a supernovae

Probing the luminosity-redshift relation of SNIa is one of the most direct measurements of cosmological expansion, and thus one of the most powerful pieces of evidence for the existence of dark energy. In our analysis we use SNIa data from the Supernova Legacy Survey (SNLS) [11], which is a dedicated SNIa survey currently including 71 SNIa in the redshift range $z = 0.2 - 1$.

4. Additional priors

In addition to the CMB, LSS and SNIa data sets mentioned above, we impose priors on the Hubble parameter, the baryon content in the universe, and the position of the LSS baryonic peak.

From the Hubble Space Telescope Key Project (HST) we have adopted a prior on the Hubble parameter of $h = 0.72 \pm 0.08$ [12]. The constraint on the baryon density today was chosen to be $\Omega_b h^2 = 0.022 \pm 0.002$ from Big Bang nucleosynthesis (BBN) [13, 14].

From the detection of baryonic acoustic oscillations (BAO) in the sample of luminous red galaxies (LRG) in the SDSS survey [15] it is also possible to put a constraint on the combination of parameters

$$A_{\text{BAO}} \equiv \left[D_M(z)^2 \frac{z}{H(z)} \right]^{1/3} \frac{\sqrt{\Omega_m H_0^2}}{z}, \quad (1)$$

where $D_M(z)$ is the comoving angular diameter distance. The BAO constraint can then be written as

$$A_{\text{BAO}} = 0.469 \left(\frac{n_s}{0.98} \right)^{-0.35} (1 + 0.94 f_\nu) \pm 0.017, \quad (2)$$

where the fit to the neutrino fraction, $f_\nu = \Omega_\nu / \Omega_m$ is given by [16]. For z we adopt the redshift of a typical LRG in the SDSS sample, $z = 0.35$. For models with non-zero α_s , we substitute n_s in eq. (2) with an effective n_s given by

$$n_{s,\text{eff}}(k_1) \equiv \left. \frac{d \ln P}{d \ln k} \right|_{k=k_1} + 1 = n_s(k_0) + \alpha_s \ln(k_1/k_0), \quad (3)$$

where P is the primordial power spectrum given by

$$\ln P = \ln A_s + (n_s - 1) \ln(k/k_0) + \alpha_s/2 \ln(k/k_0)^2, \quad (4)$$

and k_0 is set to 0.05Mpc^{-1} . We use $k_1 = 0.01 h \text{Mpc}^{-1}$, which is approximately the scale associated with the baryonic peak in the LRG sample. Our results are robust to changes of k_1 around this value, as the preferred values of α_s are small in the models considered here.

C. Parameter estimation

The parameter estimation process is based on the publicly available CosmoMC code [17], using the data and likelihoods described above.

For each model, we compute the corresponding parameter confidence intervals using three different combinations of data sets, named A, B and C (see Table I). Data set A includes the three-year WMAP data only; data set B includes also CMB data from ACBAR and BOOMERanG; and data set C also LSS and SNIa data sets and priors from HST, BBN and BAO.

As a basic six-parameter cosmological model we use the parameters $\{\Omega_b h^2, \Omega_m, \log(10^{10} A_s), h, n_s, \tau\}$. The exact parameter definitions are given by the CosmoMC code. Ω_b is the ratio of baryons to the total energy density; h is the Hubble parameter today; Ω_m is the ratio of matter to the total energy density today; A_s sets the amplitude of the primordial fluctuations; n_s is the tilt of the primordial power spectrum; and τ is the reionization optical depth.

We then extend the six-parameter model by adding the parameters $\alpha_s, r, M_\nu, \Omega_k, w$ one by one (except for α_s and r which are added simultaneously). Here, α_s is the running of n_s , defined in eq.(4); r is the ratio of tensor to scalar fluctuations; M_ν is the sum of the neutrino mass eigenstates, $M_\nu = \sum m_\nu = 93.14 \Omega_\nu h^2$; Ω_k is the amount of spatial curvature; and w is the equation of state parameter for dark energy. Finally, we vary all 11 parameters simultaneously.

For all combinations of data and parameter sets, we carry out a similar analysis both with the standard WMAP likelihood code as provided and with the two modifications described above.

Data set	Observations included
A	WMAP
B	WMAP + ACBAR + BOOMERanG
C	WMAP + ACBAR + BOOMERanG + SDSS + 2dF + SNLS + HST + BBN + BAO

TABLE I: The different combinations of data sets used in this analysis.

III. RESULTS

A. Minimal six-parameter model

We start with the simple six-parameter model having the free parameters $\{\Omega_b h^2, \Omega_m, \log(10^{10} A_s), h, n_s, \tau\}$. This was first done in ref. [3] for the combinations of data sets A and B (see Table I). For n_s they reported a $\sim 0.7\sigma$ shift to higher values when applying the modified analysis. The other parameters were only subject to small shifts of their mean values.

We repeat this analysis here, but also include data set C in the analysis. Consistent with ref. [3] we find that only n_s is notably affected by the modified likelihood, and the shift of n_s also remains for data set C, in which case the value for n_s changes from $n_s = 0.961 \pm 0.014$ to $n_s = 0.971 \pm 0.014$. This corresponds to a shift of $\sim 0.8\sigma$, and weakens the significance of $n_s \neq 1$ from ~ 2.9 to ~ 2.1 for this data set. As can be seen from refs. [2, 3], the low- l and point-source corrections contribute almost equally much to the shift in n_s . In ref. [2] they found a mean value of n_s of 0.961 when applying only the low- l corrections.

That the shift of n_s survives when adding LSS data is not very surprising; n_s is less sensitive to LSS than to CMB data because of the larger dynamic range and higher precision of the latter observations. The resulting values of n_s are summarized in Table II.

Data set	WMAP code	Modified code
A	0.954 ± 0.016	0.966 ± 0.016
B	0.958 ± 0.016	0.969 ± 0.016
C	0.961 ± 0.014	0.971 ± 0.014

TABLE II: Results for n_s in a six-parameter model. The values in the second column are found using the WMAP likelihood code, while the values in the third column are calculated using the modifications described in section II A. All errors are 1σ .

B. Running of spectral index

Next we consider how the modified WMAP likelihood affects the constraints on α_s . The simplest inflationary models predict an α_s that is slightly different from 0, and thus information on α_s can provide us with valuable information on inflationary mechanisms. Following Spergel et al. [1], we marginalize over the ratio of tensor to scalar fluctuations, r , since models with negative α_s often correspond to large tensor modes.

Our results are summarized in Table III. We find that the likelihood modifications have no major effect on the constraints on α_s , but we observe a small increase of $\sim 0.2\sigma$ in the significance of $\alpha_s \neq 0$.

Data set	WMAP code	Modified code
A	-0.050 ± 0.027	-0.052 ± 0.027
B	-0.052 ± 0.026	-0.056 ± 0.025
C	-0.013 ± 0.020	-0.014 ± 0.019

TABLE III: Estimated values for α_s from the WMAP likelihood code and our modified code. The other parameters, including r , are marginalized over.

C. Massive neutrinos

Another natural extension of the minimal six-parameter model is the addition of massive neutrinos. This is motivated by observations of neutrino oscillations, which show that neutrinos indeed are massive.

Because of their low mass, neutrinos act like a warm dark matter component in the universe. Given the energy fraction of massive neutrinos today, Ω_ν , one can easily find a limit on the sum of the neutrino masses, M_ν , by the relation $\Omega_\nu h^2 = M_\nu/93.14\text{eV}$. (See ref. [18] or [19] for a review of the cosmological properties of massive neutrinos.)

At present, the best upper limits on the absolute mass scale of neutrinos come from cosmology. The current cosmological 95% C.L. limits range from $M_\nu < 0.17\text{eV}$ [20], relying on extensive use of different data sets, to $M_\nu \lesssim 2.0\text{eV}$ for WMAP data only [1, 21, 22]. In ref. [21] they also pointed out that it will be difficult to push the upper limit on $\Omega_\nu h^2$ much below $\Omega_\nu h^2 \lesssim 0.017$ using CMB data only. This corresponds to a neutrino mass limit $M_\nu \lesssim 1.5\text{eV}$. For smaller neutrino masses, neutrinos will still be relativistic at the time of recombination, and thus the effects of the neutrino masses will not be fully revealed in the CMB power spectrum.

In our analysis we assume three species of massive neutrinos with degenerate masses. The assumption of degenerate masses has been shown to be very good for the mass regime that we are working in here [23]. The resulting neutrino mass limits are summarized in Table IV. We see that when using WMAP data alone, the upper limit on M_ν is significantly improved by the modified analysis, and that we are approaching the limit of how tight constraints on M_ν we can find from CMB data alone. If we analyze the data applying only the low- l corrections to the WMAP code, the neutrino mass limit becomes $M_\nu < 1.69\text{eV}$, which shows that both the low- l and point-source corrections are important also for this model.

Our improved M_ν limit can be understood by the slight degeneracy between the M_ν and n_s parameters, in that a larger value of n_s provides less space for a large M_ν . This can be seen from the contour plot in the M_ν - n_s plane in Figure 1. The degeneracy can be understood by the fact that both n_s and M_ν have impact on the small-scale behavior of the CMB power spectrum.

By definition, n_s sets the tilt of the primordial spectrum. If M_ν is of order $\lesssim 2\text{eV}$, it will affect the power

on scales smaller than $l \sim 300$. This happens because the perturbations of the gravitational potential on scales smaller than this are suppressed by neutrino free streaming, which in turn boosts the acoustic oscillations [24]. As M_ν increases and more of the dark matter consists of massive neutrinos, this boost of small scale power also increases. Therefore, a large value of n_s increases the power on small scales, leaving less room for M_ν to add further power without coming in conflict with data. M_ν also affects the heights of the peaks on larger scales, but this can to a large extent be compensated for by adjusting the values of Ω_m and $\Omega_b h^2$.

It is interesting to notice that the upper limit on M_ν actually weakens when we add small scale CMB data sets. From Table II we also see that the preferred value of n_s also increases when these data sets are included. This indicates that the small-scale power from ACBAR and BOOMERanG is higher than what one would expect from the WMAP data. When adding massive neutrinos to the minimal six-parameter model this increment in small-scale power can be partly accommodated by increasing M_ν instead of n_s . This will increase the small-scale power without altering the fit to the large scale spectrum.

We also see that when we add LSS and SN1a data, the neutrino mass limit is no longer affected by the modified WMAP analysis, as the additional constraints on M_ν are mainly determined by LSS data. In the LSS power spectrum neutrino free-streaming will suppress small scale power, and a larger n_s will in this case allow for a *larger* M_ν . This effect then cancels out the improved M_ν limit found from the WMAP data.

Data set	WMAP code	Modified code
A	1.90eV	1.57eV
B	2.13eV	1.72eV
C	0.45eV	0.45eV

TABLE IV: Estimated 95% C.L. upper limits on M_ν .

D. Spatial curvature

Next we add spatial curvature, Ω_k , to our six-parameter model. However, altering the geometry of universe mainly affects the positions of the CMB acoustic peaks, while the likelihood modifications mostly concern the amplitude and tilt of the power spectrum. A priori, one would therefore not expect any significant changes in Ω_k . And as seen in Table V, this is indeed the case. For all data sets, $\Omega_k = 0$ is within $\sim 1\sigma$, in good agreement with the results from the WMAP team [1].

The large improvement of the limits on Ω_k for data set C can to a large extent be understood by the well-known degeneracy between Ω_k and h , where negative values of Ω_k can be accommodated by a small h . Therefore, when

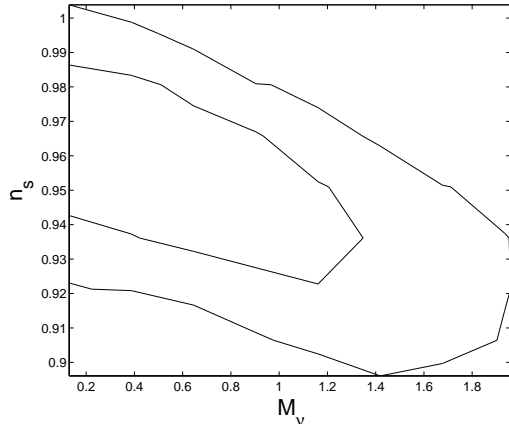


FIG. 1: 68% and 95% C.L. contours in the M_ν - n_s plane for the modified likelihood code and a seven-parameter model with free neutrino mass, using WMAP data only. There is a slight degeneracy between the two parameters, and larger values for n_s will put tighter upper limits on M_ν .

imposing the HST prior on h , the allowed range of Ω_k is significantly constrained.

Data Set	WMAP code	Modified code
<i>A</i>	$-0.057^{+0.050}_{-0.056}$	$-0.057^{+0.050}_{-0.057}$
<i>B</i>	$-0.056^{+0.052}_{-0.062}$	$-0.055^{+0.048}_{-0.055}$
<i>C</i>	-0.005 ± 0.007	-0.006 ± 0.007

TABLE V: Estimated values for Ω_k .

E. Dark energy equation of state

The nature of dark energy is one of the major questions in cosmology today. In the minimal six-parameter model, the dark energy is assumed to be a cosmological constant with $w = -1$, and this has been shown to agree well with current cosmological data (see, e.g., ref. [1]). Here we test whether the modified WMAP likelihood code alters the preferred values for w . In the following analysis we assume that w is independent of redshift.

The main effect of w on the CMB power spectrum is to shift the position of the acoustic peaks by altering the expansion history of the universe. Therefore we would not expect the limits on w to be much affected by the new WMAP likelihood analysis. Still, from Table VI we notice a small shift of order $\sim 0.2\sigma$ to smaller values of w when using CMB data only. This happens because a smaller w will enhance the late integrated Sachs-Wolfe effect, which results in a suppression of large-scale fluctuations in the observed CMB power spectrum. The slightly smaller preferred value of w in the modified analysis is accompanied by small changes also in h and Ω_m to shift

the peaks back in position. As more data is added, we see that the modified analysis has no effect on w anymore, and that a cosmological constant still fits the data.

Data set	WMAP code	Modified code
<i>A</i>	-0.98 ± 0.41	-1.05 ± 0.39
<i>B</i>	-0.97 ± 0.41	-1.03 ± 0.37
<i>C</i>	-1.00 ± 0.07	-1.00 ± 0.07

TABLE VI: Estimated values for w .

F. 11-parameter model

Finally we vary all 11 parameters $\{\Omega_b h^2, \Omega_m, \log(10^{10} A_s), h, n_s, \tau, \alpha_s, r, M_\nu, \Omega_k, w\}$ simultaneously. The results for the parameters n_s , α_s , Ω_k , w and M_ν are shown in Table VII. Here we see that all effects found in the more restricted models above are also present in this extended model.

For n_s the likelihood corrections still result in a mean value that is ~ 0.02 larger than with the original likelihood. However, as the uncertainty in n_s is increased (mainly due to a degeneracy with α_s), this shift is not as statistically significant as it was in the six-parameter model in subsection III A. Further, for data set C we see that the preferred value of n_s is in fact not much changed by the modified analysis. Rather, the power spectrum changes are accommodated by a slightly lower value of α_s to account for the smaller power for low l 's in the CMB power spectrum.

For α_s , there are no significant changes of the preferred values by the 11-parameter model, and we see that $\alpha_s = 0$ is still consistent with the data.

The same is the case for Ω_k . Here the modified analysis shifts the preferred values to slightly more negative values, but with all data sets, $\Omega_k = 0$ remains well within 1σ of its mean value.

Also for M_ν we find the same effects as above. When using CMB data only, the upper limit on M_ν is improved by the new WMAP likelihood analysis. As expected, the limit becomes weaker for the extended parameter set, but from WMAP data alone we still find a M_ν limit that is better than what is found in earlier papers, even with this large parameter space. Also, we see that the M_ν limit still becomes weaker by adding the ACBAR and BOOMERanG data sets.

For the dark energy equation of state, we still find that the modified analysis prefer slightly lower values for w . In this extended model the preferred values of w are shifted to lower values than in the more restricted model in subsection III E, which is mainly accommodated by the preferred negative value of Ω_k (as w and Ω_k shifts the positions of the acoustic peaks in opposite directions). Still $w = -1$ remains within 1σ for all of the data sets.

In Figure 2, we show the best-fit power spectrum for the 11-parameter the model both from the analysis with

the standard WMAP likelihood code and the new point-source and low- l corrected likelihood analysis. We see that the discrepancy is most notable for $l \lesssim 100$.

Parameter	WMAP code	Modified code
Data set A		
$n_s(0.05)$	0.863 ± 0.047	0.880 ± 0.046
α_s	-0.051 ± 0.029	-0.050 ± 0.029
Ω_k	$-0.019^{+0.052}_{-0.053}$	$-0.027^{+0.049}_{-0.053}$
w	-1.43 ± 1.09	-1.53 ± 1.12
M_ν	$<2.09\text{eV @ 95\% C.L.}$	$<1.66\text{eV @ 95\% C.L.}$
Data set B		
$n_s(0.05)$	0.859 ± 0.042	0.875 ± 0.041
α_s	-0.055 ± 0.027	-0.055 ± 0.027
Ω_k	$-0.010^{+0.047}_{-0.050}$	$-0.018^{+0.048}_{-0.053}$
w	-1.33 ± 1.02	-1.43 ± 1.10
M_ν	$<2.33\text{eV @ 95\% C.L.}$	$<2.02\text{eV @ 95\% C.L.}$
Data set C		
$n_s(0.05)$	0.954 ± 0.038	0.954 ± 0.036
α_s	-0.003 ± 0.028	-0.012 ± 0.026
Ω_k	-0.001 ± 0.012	$-0.001^{+0.011}_{-0.013}$
w	-1.05 ± 0.09	-1.05 ± 0.09
M_ν	$<0.51 \text{ eV @ 95\% C.L.}$	$<0.52\text{eV @ 95\% C.L.}$

TABLE VII: Parameter results for the model that includes free α_s , r , M_ν , w and Ω_k .

IV. CONCLUSION

In refs. [2] and [3], two modifications to the three-year WMAP likelihood were presented. Relative to the power spectrum presented by Hinshaw [4], they found a power deficit for low values of l due to inaccurate likelihood approximation, and a small power excess for high values of l due to over-subtracted unresolved point sources.

The impact on the inferred cosmological parameter intervals from these corrections in a minimal six-parameter model was studied in ref. [3] using CMB data only. Their single most important result was an increase in the preferred value of n_s , lowering the significance of $n_s \neq -1$ from $\sim 2.7\sigma$ to $\sim 2.0\sigma$. In the present paper, we have extended that analysis to also account for cosmological models including a non-zero running of n_s , massive neutrinos, curvature and $w \neq -1$. We have also added LSS and SNIa data sets to our analysis to see if the parameter shifts induced by the modified WMAP analysis survive when adding more data sets.

We found that the shift of n_s to larger values survives when we add LSS and SNIa data. However, when we apply all data sets in the full 11-parameter model, n_s is not affected much by the modified WMAP analysis anymore. This is mainly due to the extra freedom with α_s .

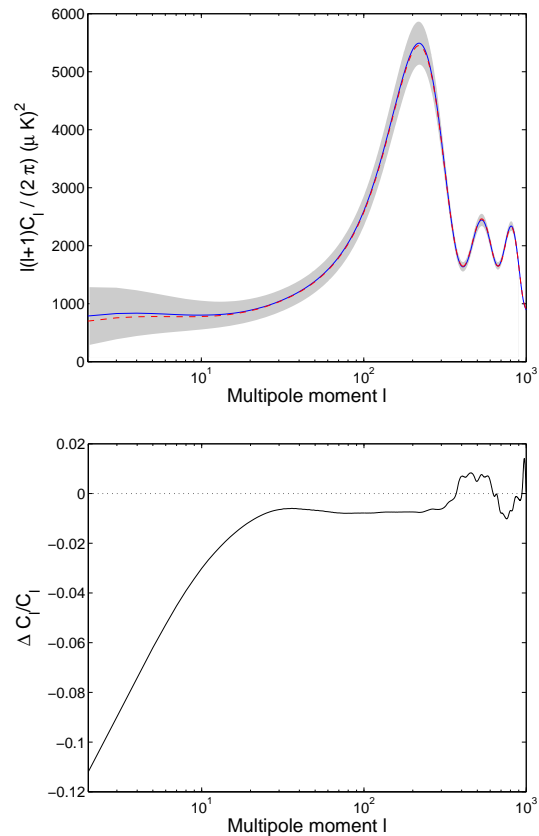


FIG. 2: Upper panel: The CMB power spectrum for the best-fit 11-parameter model with the WMAP likelihood code (solid blue line) and the low- l and point source corrected likelihood code (dashed red line). The gray shading shows the cosmic variance around the blue line. Note the small discrepancies at both low and high l 's. Lower panel: The relative difference between the two power spectra, $(C_l^{\text{modified}} - C_l^{\text{WMAP}})/C_l^{\text{WMAP}}$.

For the extended models, we found that the preferred values of α_s , Ω_k and w are not significantly affected by the modified analysis. When including massive neutrinos we found that the upper limit on M_ν when using WMAP data alone was reduced from $M_\nu < 1.90\text{eV}$ to $M_\nu < 1.57\text{eV}$. A similar improvement in the M_ν limit could not be observed when adding LSS and SNIa data, since the higher preferred value of n_s will allow for larger neutrino masses in the LSS power spectrum.

Since the initial publication of the two re-analysis papers, refs. [2] and [3], and the present paper, the WMAP team has released a new version of their likelihood code[26] that implements the suggested low- l correction and a revised point-source correction. Using this updated likelihood code, we find $n_s = 0.959 \pm 0.016$ for the six-parameter model and the WMAP data only. Including massive neutrinos, this code gives an upper bound of $M_\nu < 1.75\text{eV}$ from WMAP data only. The

difference is due to the point source amplitude and corresponding error adopted by the WMAP team, which do not match perfectly that of ref. [3]. Unfortunately, full details on the WMAP approach are not currently available, and final assessment of this issue must therefore await the release of the revised WMAP3 papers.

To conclude, the modified analysis does not strengthen the case for non-standard cosmological parameters, and the standard flat Λ CDM model still provides an excellent fit to data.

Acknowledgments

JRK and ØE acknowledge support from the Research Council of Norway through project numbers 159637 and 162830. HKE acknowledges financial support from the Research Council of Norway.

-
- [1] D. N. Spergel et al. (2006), astro-ph/0603449.
 - [2] H. K. Eriksen et al. (2006), astro-ph/0606088.
 - [3] K. M. Huffenberger, H. K. Eriksen, and F. K. Hansen (2006), astro-ph/0606538.
 - [4] G. Hinshaw et al. (2006), astro-ph/0603451.
 - [5] C.-l. Kuo et al. (ACBAR), *Astrophys. J.* **600**, 32 (2004), astro-ph/0212289.
 - [6] W. C. Jones et al., *Astrophys. J.* **647**, 823 (2006), astro-ph/0507494.
 - [7] F. Piacentini et al., *Astrophys. J.* **647**, 833 (2006), astro-ph/0507507.
 - [8] T. E. Montroy et al., *Astrophys. J.* **647**, 813 (2006), astro-ph/0507514.
 - [9] M. Colless et al. (2003), astro-ph/0306581.
 - [10] M. Tegmark et al. (SDSS), *Astrophys. J.* **606**, 702 (2004), astro-ph/0310725.
 - [11] P. Astier et al., *Astron. Astrophys.* **447**, 31 (2006), astro-ph/0510447.
 - [12] W. L. Freedman et al., *Astrophys. J.* **553**, 47 (2001), astro-ph/0012376.
 - [13] S. Burles, K. M. Nollett, and M. S. Turner, *Phys. Rev.* **D63**, 063512 (2001), astro-ph/0008495.
 - [14] R. H. Cyburt, *Phys. Rev.* **D70**, 023505 (2004), astro-ph/0401091.
 - [15] D. J. Eisenstein et al., *Astrophys. J.* **633**, 560 (2005), astro-ph/0501171.
 - [16] A. Goobar, S. Hannestad, E. Mortsell, and H. Tu (2006), astro-ph/0602155.
 - [17] A. Lewis and S. Bridle, *Phys. Rev.* **D66**, 103511 (2002), astro-ph/0205436.
 - [18] O. Elgaroy and O. Lahav, *New J. Phys.* **7**, 61 (2005), hep-ph/0412075.
 - [19] J. Lesgourgues and S. Pastor, *Phys. Rept.* **429**, 307 (2006), astro-ph/0603494.
 - [20] U. Seljak, A. Slosar, and P. McDonald (2006), astro-ph/0604335.
 - [21] K. Ichikawa, M. Fukugita, and M. Kawasaki, *Phys. Rev.* **D71**, 043001 (2005), astro-ph/0409768.
 - [22] M. Fukugita, K. Ichikawa, M. Kawasaki, and O. Lahav, *Phys. Rev.* **D74**, 027302 (2006), astro-ph/0605362.
 - [23] A. Slosar, *Phys. Rev.* **D73**, 123501 (2006), astro-ph/0602133.
 - [24] S. Dodelson, E. Gates, and A. Stebbins, *Astrophys. J.* **467**, 10 (1996), astro-ph/9509147.
 - [25] <http://lambda.gsfc.nasa.gov>; version v2p1.
 - [26] Version v2p2p1